

# Stable Bound Orbits of Massless Particles around a Black Ring

<sup>1,2</sup>Takahisa Igata,<sup>\*</sup> <sup>2</sup>Hideki Ishihara,<sup>†</sup> and <sup>2</sup>Yohsuke Takamori<sup>‡</sup>

<sup>1</sup>*Department of Physics, Kinki University, Osaka 577-8502, Japan*

<sup>2</sup>*Department of Mathematics and Physics, Graduate School of Science,  
Osaka City University, Osaka 558-8585, Japan*

We study the geodesic motion of massless particles in singly rotating black ring spacetimes. We find stable stationary orbits of massless particles in toroidal spiral shape in the case that the thickness parameter of a black ring is less than a critical value. Furthermore, there exist nonstationary massless particles bounded in a finite region outside the horizon. This is the first example of stable bound orbits of massless particles around a black object.

PACS numbers: 04.50.Gh

## I. INTRODUCTION

Higher-dimensional black holes gather much attention in the context of modern unified theories of interactions (see for a review [1]). It is understood that the higher-dimensional black holes are very different from the four-dimensional ones in some aspects. In four dimensions, stationary black holes in a vacuum must have spherical horizons, and are uniquely characterized by their mass and angular momentum. In higher dimensions, however, black holes with unusual horizon topology exist in addition to black holes with spherical horizon topology [2]. The first discovery of the black hole solutions with  $S^2 \times S^1$  topology, black ring solutions, was made in five dimensions by Emparan and Reall [3]. The black ring solutions reveal that a black hole in a vacuum is not uniquely characterized only by its mass and angular momenta in higher dimensions. After this pioneering work, various types of black ring solutions have been found by many authors [4–10]. It is important to study their geometrical properties and physical phenomena that occur around each of them in order to understand the differences between black holes and black rings.

---

<sup>\*</sup>Electronic address: igata@sci.osaka-cu.ac.jp

<sup>†</sup>Electronic address: ishihara@sci.osaka-cu.ac.jp

<sup>‡</sup>Electronic address: takamori@sci.osaka-cu.ac.jp

One of the important steps to clarify the geometry of spherical black holes and black rings is the studies of geodesics in these spacetimes. For example, the separability in the Hamilton-Jacobi equation for geodesic motion, which is a general property in arbitrary-dimensional Myers-Perry black holes [11], implies that the black holes have the hidden symmetries called Killing tensors. On the other hand, in the case of singly rotating black rings, such separation of variables occurs for some special cases of geodesics: the geodesics on the rotational axis or the equatorial plane, and the geodesics for the massless particles with zero-energy [12, 13]. Recently, the Hamilton-Jacobi equation in these separable cases were solved analytically [14, 15].

In four dimensions, a massive particle moving around a black hole has two types of orbits: bound orbits by the gravitational force, and unbound ones. A part of bound orbits are bounded in a region outside the black hole horizon, where the centrifugal force prevents the particles from falling into the horizon. There are circular orbits that are stable against small perturbations as special cases of the bounded orbits. In contrast, there is no stable circular orbit of massive particles in higher-dimensional Schwarzschild black holes, nor at least on the equatorial planes in the five-dimensional Myers-Perry black holes [11]. This fact is completely different from the four-dimensional case. However, stable bound orbits of massive particles exist around a black ring if the thickness parameter is less than a critical value [16]. The result suggests that we can distinguish a black ring from a spherical black hole with the same mass and the same angular momentum by the orbits of massive particles. Furthermore, it is shown that chaotic motion of massive particles appears [17]. It indicates that there is not the sufficient number of constants of motion for integration of geodesic equations for a massive particle in black ring spacetimes.

How about massless particles? In four-dimensional black holes, there exists no bounded orbit of massless particles in a finite region outside the horizon though there are unstable circular orbits of massless particles. Higher-dimensional spherical black holes with the asymptotic flatness would have the same property as the four-dimensional ones. In contrast, in black holes with the asymptotic structure of the Kaluza-Klein type [18–20], a massless particle with nonvanishing momenta in the directions of extra dimensions could be bounded in a finite region. The most simple example of such nonasymptotically flat black holes is a black string with periodic identification along the string direction. The geometry is given by the direct product of a Schwarzschild spacetime with a one-dimensional circle,  $S^1$ . A massless particle that has nonvanishing momentum along  $S^1$  behaves as a massive particle in the four-dimensional Schwarzschild spacetime. Hence, such a massless particle can be bounded around the black string.

Are there bounded orbits of massless particles around a black ring? On the one hand, since

a black ring spacetime is asymptotically flat, it seems that massless particles cannot be bounded around it. On the other hand, since the geometry of a black ring approaches the one of a black string in a region near the horizon, then we expect that a massless particle could be bounded around it if the particle had nonvanishing angular momenta in two independent angular directions.

In this paper, we investigate null geodesics in the singly rotating black ring geometry in five dimensions as a moving particle system in a two-dimensional potential. We show the existence of stable bound orbits of massless particles and the existence of bounded orbits of massless particles generally in a finite region outside the horizon.

The paper is organized as follows. The following section provides the singly rotating black ring geometry and the Hamilton formalism for a massless particle around a black ring. In Sec. III, we show the existence of stable bound orbits of massless particles in the case that the black ring thickness parameter is smaller than a critical value. Section IV shows that there exist more general orbits of massless particles bounded in a finite domain outside the black ring horizon.

## II. HAMILTONIAN FOR A MASSLESS PARTICLE

### A. Geometry of singly rotating black rings

We consider the metric of singly rotating black rings given by

$$\begin{aligned} ds^2 &= g_{\alpha\beta} dx^\alpha dx^\beta \\ &= -\frac{F(y)}{F(x)} \left( dt - CR \frac{1+y}{F(y)} d\psi \right)^2 \\ &\quad + \frac{R^2}{(x-y)^2} F(x) \left( -\frac{G(y)}{F(y)} d\psi^2 - \frac{dy^2}{G(y)} + \frac{dx^2}{G(x)} + \frac{G(x)}{F(x)} d\phi^2 \right), \end{aligned} \quad (1)$$

with

$$F(\xi) = 1 + \lambda\xi, \quad G(\xi) = (1 - \xi^2)(1 + \nu\xi), \quad (2)$$

$$C = \sqrt{\lambda(\lambda - \nu) \frac{1 + \lambda}{1 - \lambda}}, \quad (3)$$

where the ranges of the ring coordinates  $x$  and  $y$  are given by

$$-1 \leq x \leq 1 \quad \text{and} \quad -\infty \leq y \leq -1, \quad (4)$$

and the angular coordinates  $\phi$  and  $\psi$  are periodic in  $2\pi$ . The parameter  $R$  denotes the radius of the black ring. The parameters  $\nu$  and  $\lambda$  describe the thickness of the black ring and the rotational

velocity in the  $\psi$ -direction through  $C$ , respectively. These parameters should be chosen in the range

$$0 < \nu \leq \lambda < 1, \quad (5)$$

and related as

$$\lambda = \frac{2\nu}{1 + \nu^2} \quad (6)$$

to avoid the conical singularities at  $x = \pm 1$  and  $y = -1$ . The event horizon and the ergosurface in the  $S^2 \times S^1$  topology are located at  $y = -1/\nu$  and  $y = -1/\lambda$ , respectively.

## B. Hamiltonian formalism

Throughout this paper, we use the Hamiltonian formalism for a massless particle. Motion of a massless particle is governed by the Hamiltonian,

$$H = \frac{1}{2} g^{\alpha\beta} k_\alpha k_\beta, \quad (7)$$

with the null condition

$$g^{\alpha\beta} k_\alpha k_\beta = 0, \quad (8)$$

where  $k_\alpha$  is the canonical momentum. For the black rings,  $g^{\alpha\beta}$  is given by the inverse of Eq. (1).

Since the metric (1) admits three Killing vectors,  $\partial_t$ ,  $\partial_\psi$ , and  $\partial_\phi$ , there exist three constants of motion,

$$E = -k_t, \quad L_\psi = k_\psi, \quad \text{and} \quad L_\phi = k_\phi, \quad (9)$$

where  $E$ ,  $L_\psi$ , and  $L_\phi$  are energy, angular momenta in the  $\psi$ - and the  $\phi$ -direction of a massless particle, respectively. Substituting Eqs. (9) into Eq. (7), we obtain the two-dimensional effective Hamiltonian,

$$H = \frac{1}{2} (g^{xx} k_x^2 + g^{yy} k_y^2 + E^2 U), \quad (10)$$

where  $U$  is the effective potential given by

$$U = g^{tt} + g^{\phi\phi} l_\phi^2 + g^{\psi\psi} l_\psi^2 - 2g^{t\psi} l_\psi, \quad (11)$$

with

$$\begin{aligned} g^{tt} &= -\frac{F(x)}{F(y)} - \frac{C^2(x-y)^2(y+1)^2}{G(y)F(x)F(y)}, & g^{xx} &= \frac{(x-y)^2}{R^2} \frac{G(x)}{F(x)}, & g^{yy} &= -\frac{(x-y)^2}{R^2} \frac{G(y)}{F(x)}, \\ g^{\phi\phi} &= \frac{(x-y)^2}{R^2 G(x)}, & g^{\psi\psi} &= -\frac{F(y)(x-y)^2}{R^2 G(y)F(x)}, & g^{t\psi} &= -\frac{C(x-y)^2(y+1)}{RG(y)F(x)}. \end{aligned} \quad (12)$$

In Eq. (11), we have introduced the normalized angular momenta,  $l_\phi := L_\phi/E$  and  $l_\psi := L_\psi/E$ .

The equations of motion for Eq. (10) are

$$\dot{x}^i = g^{ij} k_j, \quad (i, j = x, y), \quad (13)$$

$$\dot{k}_i = -\frac{1}{2}(\partial_i g^{jk} k_j k_k + \partial_i U), \quad (14)$$

where the overdot denotes the differentiation with respect to an affine parameter on each world line of the massless particle. The null condition (8) becomes

$$g^{xx} k_x^2 + g^{yy} k_y^2 + E^2 U = 0. \quad (15)$$

Note that the effective potential (11) is symmetric with respect to  $l_\phi \rightarrow -l_\phi$ , whereas asymmetric with respect to  $l_\psi \rightarrow -l_\psi$ , because the black ring described by the metric (1) rotates only in the  $\psi$ -direction. Therefore, we assume  $l_\phi \geq 0$  without loss of generality in what follows. Further, we consider future-directed null geodesics with positive energy  $E > 0$ .

### III. TOROIDAL SPIRAL ORBITS

In this section, we discuss the existence of local minimum points of the effective potential  $U$ . In the case  $U = 0$  at the points, they correspond to stable stationary orbits of massless particles.

Throughout the following discussion we use the new coordinates  $(\zeta, \rho)$  defined by

$$\zeta = \frac{R\sqrt{y^2-1}}{x-y} \quad \text{and} \quad \rho = \frac{R\sqrt{1-x^2}}{x-y}. \quad (16)$$

Figure 1 shows the relations of  $(x, y)$  and  $(\zeta, \rho)$ . The new coordinate system has an advantage because the metric is written in the well known form,  $ds^2 = -dt^2 + d\zeta^2 + \zeta^2 d\psi^2 + d\rho^2 + \rho^2 d\phi^2$ , in the flat limit of Eq. (1). In what follows we employ the unit  $R = 1$  for simplicity.

We consider the special stationary motion that satisfies  $\dot{\zeta} = \dot{\rho} = 0$  and  $\dot{k}_\zeta = \dot{k}_\rho = 0$ , or equivalently,  $\dot{x} = \dot{y} = 0$  and  $\dot{k}_x = \dot{k}_y = 0$ . Then the equations of motion (13) and (14) lead to  $k_\zeta = k_\rho = 0$  and the stationary point conditions for  $U$ ,

$$\partial_\zeta U = \partial_\rho U = 0, \quad (17)$$

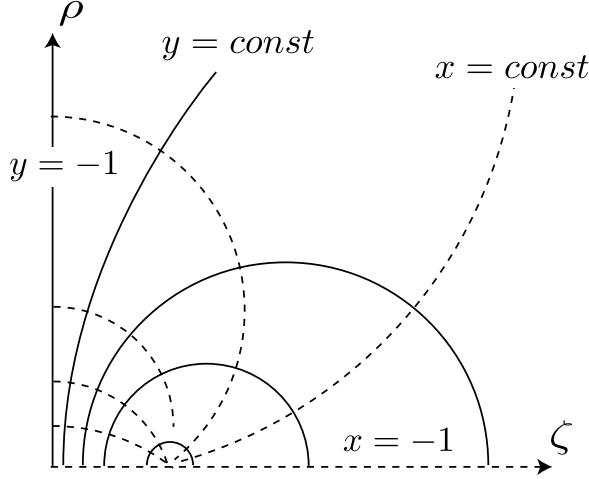


FIG. 1: Relation of the  $(x, y)$  coordinates and the  $(\zeta, \rho)$  coordinates. The solid curves denote  $y = \text{const}$ , and the dashed curves denote  $x = \text{const}$  in the  $\zeta$ - $\rho$  plane.

where  $U$  is the function of  $\zeta$  and  $\rho$  given by Eq. (11) as  $U = U(x(\zeta, \rho), y(\zeta, \rho))$ . Furthermore, from the null condition (15),  $U$  must satisfy

$$U = 0. \quad (18)$$

The stationary orbits of massless particles satisfying Eqs. (17) and (18) with nonvanishing  $E$ ,  $l_\psi$ , and  $l_\phi$ , are tangent to the null Killing vectors that are linear combinations of  $\partial_t$ ,  $\partial_\phi$ , and  $\partial_\psi$ . Hence, the projection of the orbit on a  $t = \text{const}$  surface makes a toroidal spiral curve on a two-dimensional torus, a direct product of  $S^1$  with a constant radius  $\zeta$  generated by  $\partial_\psi$  and  $S^1$  with a constant radius  $\rho$  generated by  $\partial_\phi$ . Then, we call such a stationary orbit a *toroidal spiral orbit* of a massless particle.

#### A. Set of Stationary points

Since  $U$  includes the two parameters  $l_\phi$  and  $l_\psi$ , then it is useful to consider the direct product space: the two-dimensional space of  $(\zeta, \rho)$  times the two-dimensional parameter space of  $(l_\psi, l_\phi)$ , i.e., the four-dimensional space defined as  $\mathcal{N} = \{(\zeta, \rho, l_\psi, l_\phi)\}$ . In  $\mathcal{N}$ , Eqs. (17) defines a two-dimensional surface, say  $\Sigma$ , which represents the set of stationary points.

We consider the restriction of  $U$  to  $\Sigma$ , denoted by  $U|_\Sigma$ . The condition

$$U|_\Sigma = 0 \quad (19)$$

makes a curve on  $\Sigma$ , and each point on the curve corresponds to a stationary orbit of a massless

particle of  $\zeta = \text{const}$  and  $\rho = \text{const}$ , i.e., a stationary toroidal spiral orbit. In particular, if a point on  $\Sigma$  satisfying the condition (19) is a local minimum of  $U$ , the corresponding stationary toroidal spiral orbit is stable. The condition for a stationary point of  $U$  to be a local minimum is

$$\det \mathcal{H}(U)|_{\Sigma} > 0 \quad \text{and} \quad \text{tr} \mathcal{H}(U)|_{\Sigma} > 0 \quad (20)$$

at the point, where  $\mathcal{H}(U)|_{\Sigma}$  is the restriction of the Hessian matrix of  $U$ ,

$$\mathcal{H}(U) = \begin{pmatrix} \partial_{\zeta}^2 U & \partial_{\zeta} \partial_{\rho} U \\ \partial_{\rho} \partial_{\zeta} U & \partial_{\rho}^2 U \end{pmatrix}, \quad (21)$$

to  $\Sigma$ . In order to seek local minimum points of  $U$  satisfying Eq. (19), we find  $\Sigma$  first, and then we inspect the conditions (19) and (20).

Here, we study the surface  $\Sigma$  in detail. Equations (17) yield the quadratic equation in  $l_{\psi}$ ,

$$\alpha l_{\psi}^2 + 2\beta l_{\psi} + \gamma = 0, \quad (22)$$

where  $\alpha$ ,  $\beta$ , and  $\gamma$  are the functions of  $\zeta$  and  $\rho$  given by

$$\alpha = \partial_{\rho} g^{\psi\psi} - \frac{\partial_{\rho} g^{\phi\phi} \partial_{\zeta} g^{\psi\psi}}{\partial_{\zeta} g^{\phi\phi}}, \quad (23)$$

$$\beta = -\partial_{\rho} g^{t\psi} + \frac{\partial_{\rho} g^{\phi\phi} \partial_{\zeta} g^{t\psi}}{\partial_{\zeta} g^{\phi\phi}}, \quad (24)$$

$$\gamma = \partial_{\rho} g^{tt} - \frac{\partial_{\rho} g^{\phi\phi} \partial_{\zeta} g^{tt}}{\partial_{\zeta} g^{\phi\phi}}. \quad (25)$$

We can solve Eq. (22) with respect to  $l_{\psi}$  as the function of  $\zeta$  and  $\rho$  on  $\Sigma$  in the form

$$l_{\psi}^{\pm} = \frac{-\beta \pm \sqrt{\beta^2 - \alpha\gamma}}{\alpha}, \quad (26)$$

and these lead to  $l_{\phi}^{\pm}$  satisfying Eqs. (17), respectively. Therefore, there exist two branches of  $\Sigma$ ,  $\Sigma^+ = \{(\zeta, \rho, l_{\psi}^+(\zeta, \rho), l_{\phi}^+(\zeta, \rho))\}$  and  $\Sigma^- = \{(\zeta, \rho, l_{\psi}^-(\zeta, \rho), l_{\phi}^-(\zeta, \rho))\}$ . They are projected uniquely into domains where  $l_{\psi}^{\pm}(\zeta, \rho)$  and  $l_{\phi}^{\pm}(\zeta, \rho)$  take real values in the  $\zeta$ - $\rho$  plane.

## B. The case $\nu = 0.1$

We discuss the existence of stationary toroidal spiral orbits of massless particles in the black ring spacetime with  $\nu = 0.1$  as an example. We take  $\Sigma^-$  first, and consider the contours  $U|_{\Sigma^-} = 0$  and  $\det \mathcal{H}(U)|_{\Sigma^-} = 0$  on it. The surface  $\Sigma^-$  with the contours is uniquely projected into the  $\zeta$ - $\rho$  plane as shown in Fig. 2(a). The contours  $U|_{\Sigma^-} = 0$  and  $\det \mathcal{H}(U)|_{\Sigma^-} = 0$  intersect at the points p and

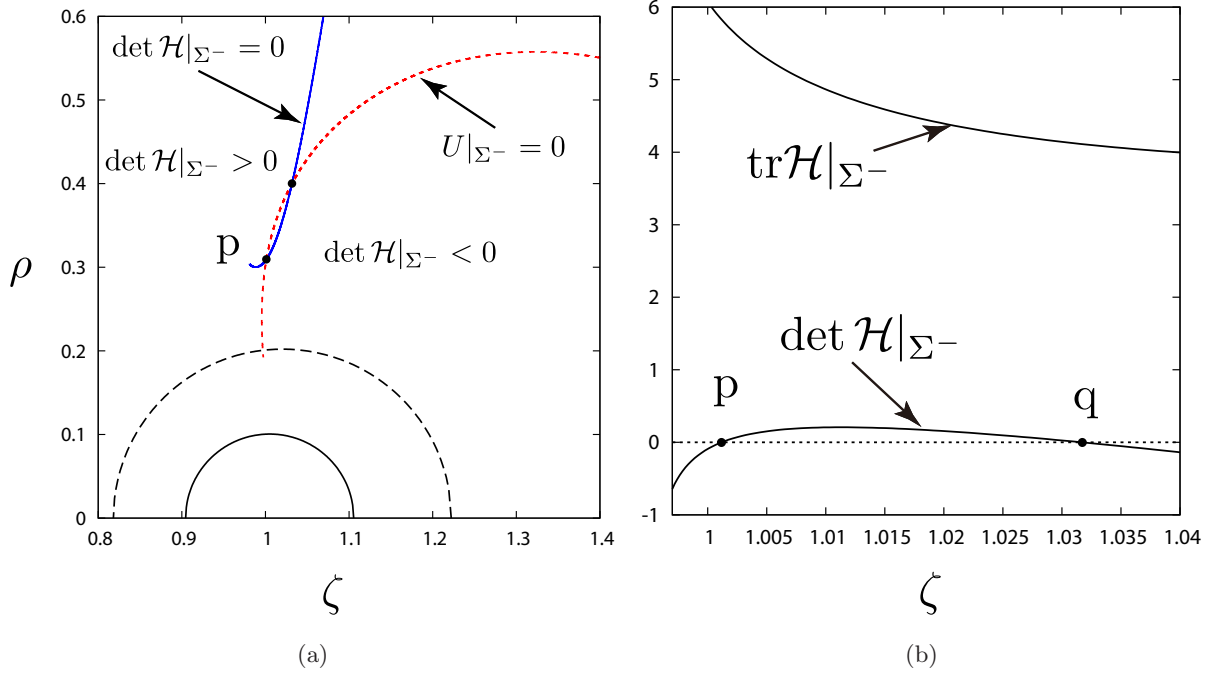


FIG. 2: (a) The contours of  $\det \mathcal{H}|_{\Sigma^-} = 0$  ((blue) solid curve) and  $U|_{\Sigma^-} = 0$  ((red) dashed curve) on  $\Sigma^-$  are projected on the  $\zeta$ - $\rho$  plane in the case of the black ring with  $\nu = 0.1$ . The solid half circle and the dashed half circle on the horizontal axis represent the event horizon and the ergosurface of the black ring, respectively. (b) Plots of the value of  $\det \mathcal{H}|_{\Sigma^-}$  and  $\text{tr} \mathcal{H}|_{\Sigma^-}$  as the functions of  $\zeta$  along the contour  $U|_{\Sigma^-} = 0$ .

q, and the segment of  $U|_{\Sigma^-} = 0$  between p and q is in the region  $\det \mathcal{H}(U)|_{\Sigma^-} > 0$ . We can check  $\text{tr} \mathcal{H}(U)|_{\Sigma^-} > 0$  on the segment separately as seen in Fig. 3(b). As will be seen later, both of  $l_\psi^-$  and  $l_\phi^-$  are nonvanishing on the segment, and then stable toroidal spiral orbits of massless particles are realized at any points on the segment. The stable toroidal spiral orbits make a one-parameter family along the segment.

The stability condition is marginally satisfied at the points p and q. It means that there exist two marginally stable toroidal spiral orbits similar to the *Innermost Stable Circular Orbit* (ISCO) of a massive particle moving around a black hole in four dimensions. The point p, near the event horizon, corresponds to the *Innermost Stable Toroidal Spiral Orbit* (ISTSO) for a massless particle in the black ring spacetime, and the other point q is the *Outermost Stable Toroidal Spiral Orbit* (OSTSO) for a massless particle in the black ring spacetime. By the same analysis, no stable toroidal spiral orbit appears in the other branch  $\Sigma^+$  for  $\nu = 0.1$ . For thinner black rings, stable toroidal spiral orbits would be found in both the branches.

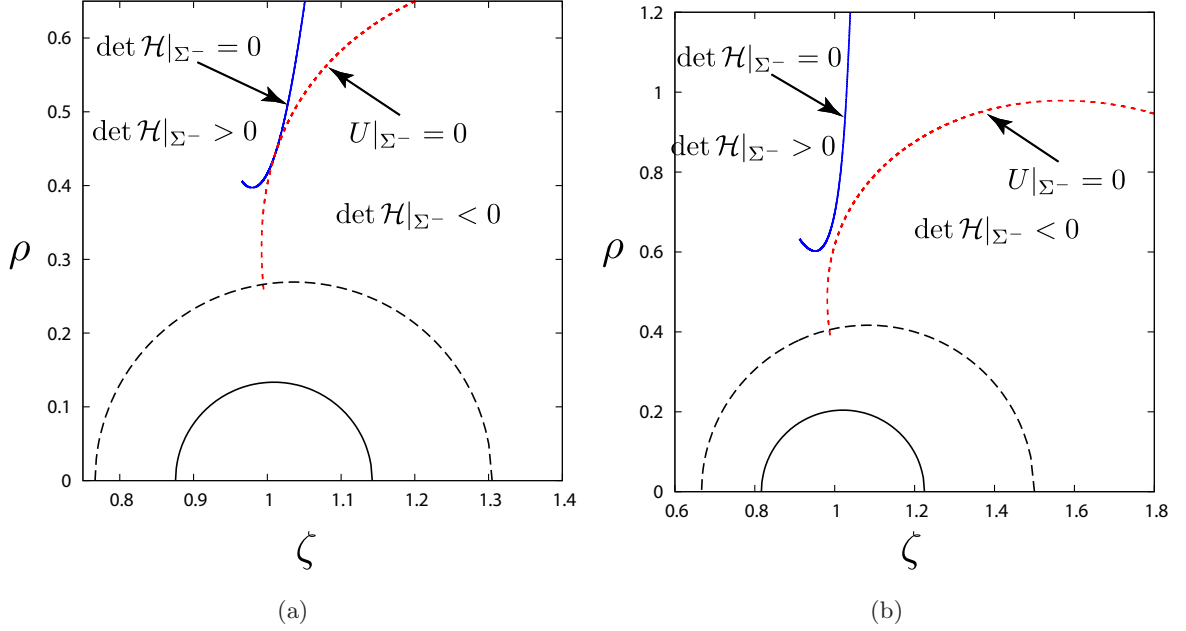


FIG. 3: The (blue) solid curve and the (red) dashed curve in each panel are the projected contours of  $\det \mathcal{H}|_{\Sigma^-} = 0$  and  $U|_{\Sigma^-} = 0$  on the  $\zeta$ - $\rho$  plane, respectively, in the cases (a)  $\nu = 0.13224 \simeq \nu_c$  and (b)  $\nu = 0.2$ . The solid half circle and the dashed half circle on the horizontal axis in each panel represent the event horizon and the ergosurface of the black ring, respectively.

### C. Critical value of $\nu$

We discuss the thickness parameter  $\nu$  with which the black ring has the stable toroidal spiral orbits of massless particles. Numerical analysis shows that the crossing points p and q of contours  $U|_{\Sigma^-} = 0$  and  $\det \mathcal{H}(U)|_{\Sigma^-} = 0$  approach each other as  $\nu$  increases. The points p and q merge together when  $\nu$  takes a critical value  $\nu_c$ , and the crossing points disappear for  $\nu > \nu_c$ .

Figure 3 shows the projection of  $U|_{\Sigma^-} = 0$  and  $\det \mathcal{H}(U)|_{\Sigma^-} = 0$  into the  $\zeta$ - $\rho$  plane for the cases (a)  $\nu = 0.13224$  and (b)  $\nu = 0.2$ . In the former case, the curve of  $U|_{\Sigma^-} = 0$  is tangent to the one of  $\det \mathcal{H}|_{\Sigma^-} = 0$  at a point, that is, the points p and q merge together. Hence, the critical value of  $\nu$  is approximately given by  $\nu_c = 0.13224 \dots$ . The condition to determine the critical value  $\nu_c$  is discussed in Appendix A. On the other hand, the contours  $U|_{\Sigma^-} = 0$  and  $\det \mathcal{H}(U)|_{\Sigma^-} = 0$  have no crossing point in the case  $\nu = 0.2$ . For the thin black rings with  $\nu \leq \nu_c$ , there exist stable toroidal spiral orbits of massless particles, while for the black ring with  $\nu > \nu_c$  toroidal spiral orbits become unstable.

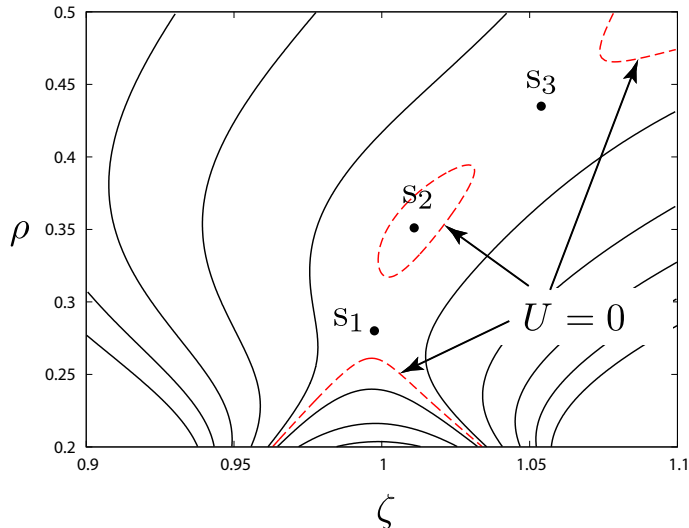


FIG. 4: Contour plot of the effective potential  $U$  with  $l_\psi = -1.2651$  and  $l_\phi = 0.5204$  for  $\nu = 0.1$ . The (red) dashed lines indicate the contour of  $U = 0$ . The point  $s_2$  is a local minimum, and  $s_1$  and  $s_3$  are saddle points.

#### IV. BOUNDED ORBITS OF MASSLESS PARTICLES

In this section, we consider nonstationary motion of massless particles trapped in a bounded domain outside the black ring horizon. It is natural to consider that there exist orbits wandering around the stable toroidal spiral orbits, which are discussed in the previous section. Such bounded orbits appear if particles are confined by an effective potential barrier. Since massless particles must satisfy the null condition (15), the contour  $U = 0$  is a set of turning points. Therefore, if a potential minimum with  $U < 0$  is surrounded by a closed contour  $U = 0$  outside the horizon, then bounded orbits exist. This is a sufficient condition for the existence of the bounded orbits.

Figure 4 shows contours of a typical  $U$  that has a negative local minimum surrounded by the closed contour of  $U = 0$  in the case  $\nu = 0.1$ . Massless particles are confined inside the potential barrier around a negative local minimum  $s_2$ . Indeed, we can verify that such a orbit is bounded by the closed contour  $U = 0$  by the numerical integration of the null geodesic equations (13) and (14).

Figure 5 shows the projection of the contours  $\det \mathcal{H}(U)|_{\Sigma^-} = 0$  and  $U|_{\Sigma^-} = 0$  into the  $l_\psi$ - $l_\phi$  plane. A cusp of the projection of  $\det \mathcal{H}(U)|_{\Sigma^-} = 0$  appears (see Fig. 5(a)). The projection of  $U|_{\Sigma^-} = 0$  has a self-intersecting point, r, and two cusps, p and q, on the projection of  $\det \mathcal{H}|_{\Sigma^-} = 0$  (see Fig. 5(b)). These results mean that the embedding of  $\Sigma^-$  is threefold. In fact, Figs. 6 show that a part of  $\Sigma^-$  in the three-dimensional space of  $(\rho, l_\psi, l_\phi)$  is threefold. The contour  $\det \mathcal{H}(U)|_{\Sigma^-} = 0$

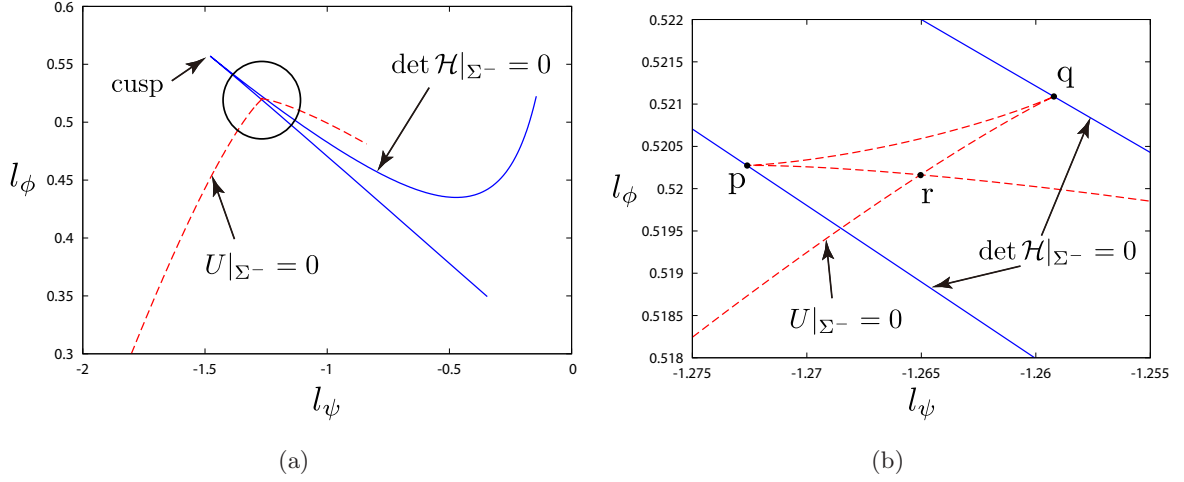


FIG. 5: (a) Projection of the contours  $\det \mathcal{H}|_{\Sigma^-} = 0$  and  $U|_{\Sigma^-} = 0$  into the  $l_\psi$ - $l_\phi$  plane in the case  $\nu = 0.1$ . The projection of the contour  $\det \mathcal{H}|_{\Sigma^-} = 0$  is shown by the (blue) solid curve, and the contour  $U|_{\Sigma^-} = 0$  is shown by the (red) dashed curve. There is a cusp on the projection of the contour  $\det \mathcal{H}|_{\Sigma^-} = 0$ , and  $\det \mathcal{H}|_{\Sigma^-} > 0$  inside the wedge. (b) A close-up view of the area inside the circle in the panel (a).

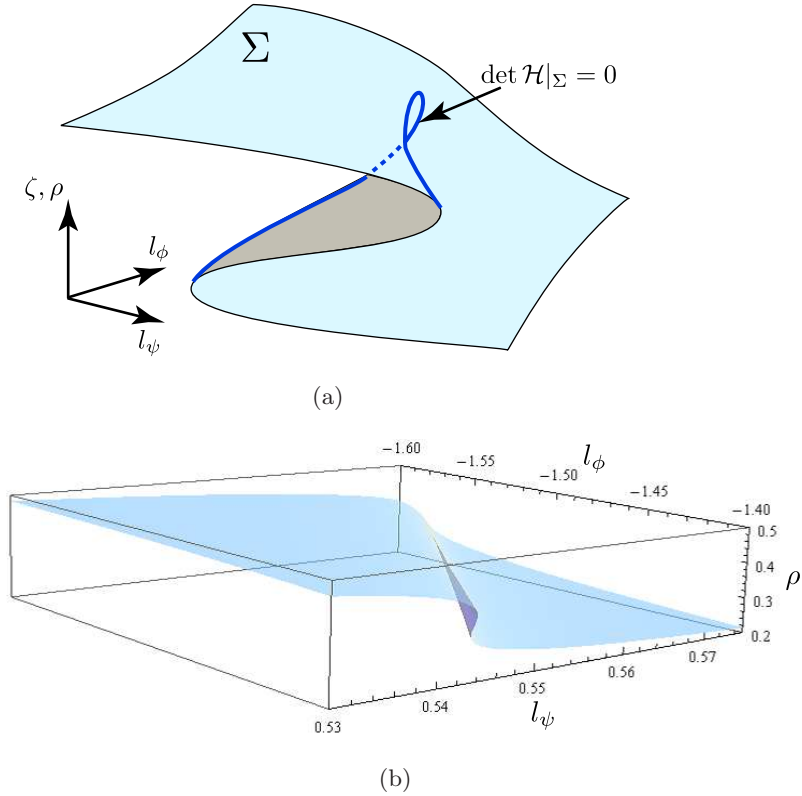


FIG. 6: (a) Schematic diagram of the surface  $\Sigma$ . The contour of  $\det \mathcal{H} = 0$  is drawn by a solid curve. (b) Numerical plot of  $\Sigma^-$  in the three-dimensional space  $(\rho, l_\psi, l_\phi)$  in the case  $\nu = 0.1$ .

stationary points		$\det \mathcal{H} _{\Sigma^-}$	$U _{\Sigma^-}$
$t_1$	$s_1$	$-$	$+$
	$s_1$	$-$	$+$
$t_2$	$s_2$	$+$	$-$
	$s_3$	$-$	$-$
$t_3$	$s_1$	$-$	$+$
	$s_2$	$+$	$-$
	$s_3$	$-$	$+$
$t_4$	$s_1$	$-$	$+$
	$s_2$	$+$	$0$
	$s_3$	$-$	$+$
$t_5$	$s_1$	$-$	$+$
	$s_2$	$+$	$+$
	$s_3$	$-$	$+$
$t_6$	$s_3$	$-$	$+$

TABLE I: A variety of stationary points. The symbols  $\pm$  show that  $\det \mathcal{H}|_{\Sigma^-}$  and  $U|_{\Sigma^-}$  take a positive or a negative value, respectively.

makes the folded line, and hence the cusps and the crossing point on the  $l_\psi$ - $l_\phi$  plane are regular points on  $\Sigma^-$ .

In order to understand variety of the potential shapes that are dependent on the parameters  $l_\psi$  and  $l_\phi$ , we consider several representative points,  $t_1$ - $t_6$ , in the  $l_\psi$ - $l_\phi$  plane as shown in Fig. 7. For each set of the parameters  $(l_\psi, l_\phi)$  in the onefold region of  $\Sigma^-$ , outside the wedge of  $\det \mathcal{H}(U)|_{\Sigma^-} = 0$ ,  $t_1$  or  $t_6$  for example, the stationary point of  $U$  is a saddle point because  $\det \mathcal{H}(U)|_{\Sigma^-} < 0$  (see Table I). On the other hand, for each set of the parameters  $(l_\psi, l_\phi)$  in the threefold region, inside the wedge,  $t_2$ - $t_5$  for example, there exist three stationary points of  $U$ , two saddles and one local minimum. In particular, if we take a point in the triangle-like region qpr enclosed by the projection of  $U|_{\Sigma^-} = 0$ ,  $t_3$  for example,  $U < 0$  at the local minimum, and  $U > 0$  at the two saddle points. In this case, the local minimum point is surrounded by a closed contour of  $U = 0$  (see Fig. 7), and then there exist bounded orbits of massless particles around the local minimum point.

A point on the projected segment of  $U|_{\Sigma^-} = 0$  between p and q, e.g.,  $t_4$ , means that the effective potential admits stable toroidal spiral orbits, which are specified by a parameter, e.g.,  $l_\psi$ , on the segment. A point on the segment between p and r or between q and r implies the potential well of  $U$  from which massless particles can marginally leak out through the saddle point. The points p and q correspond to the ISTSO and the OSTSO, respectively. The effective potential at the point r has two marginally leaking saddle points with  $U|_{\Sigma^-} = 0$ . In the case  $\nu = \nu_c$ , the projection of

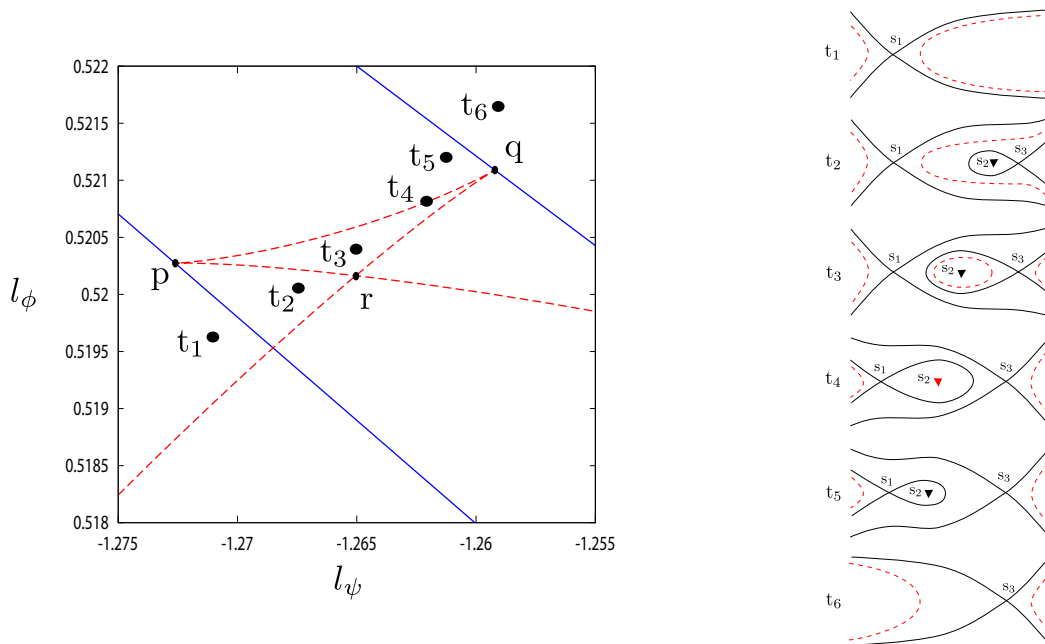


FIG. 7: Schematic view of stationary points. Typical sets of parameters  $(l_\psi, l_\phi)$  are shown by points  $t_1$ – $t_6$  in the  $l_\psi$ – $l_\phi$  plane (the left panel). The effective potentials corresponding to  $t_1$ – $t_6$  are shown by contour plots (the right panel). The solid lines are the contours of  $U$  that are through saddle points, and the (red) dashed lines are the contours of  $U = 0$ . The solid triangles show the local minimum points.

$U|_{\Sigma^-} = 0$  passes through the cusp of the projection of  $\det \mathcal{H}(U)|_{\Sigma^-} = 0$  on the  $l_\psi$ – $l_\phi$  plane, and then the triangle region  $qpr$  shrinks to a point. Thus, there is no stable bound orbit of massless particles for the black rings with  $\nu > \nu_c$ .

## V. SUMMARY

We have investigated null geodesics in the singly rotating black ring geometry in five dimensions. As a result, we have found stable stationary orbits of massless particles in toroidal spiral shape if the thickness parameter  $\nu$  is less than the critical value  $\nu_c = 0.13224 \dots$ . The stable toroidal spiral orbits are a one-parameter family of the solutions characterized by a combination of the two nonvanishing angular momenta divided by the energy. As marginally stable orbits, there exist the innermost stable toroidal spiral orbit and the outermost stable toroidal spiral orbit. We have also shown the existence of nonstationary motion of massless particles trapped in a bounded domain outside the black ring horizon.

In four-dimensional black hole spacetimes, there exist stable stationary timelike geodesics like planetary orbits. In five dimensions, in contrast, spherical black holes with the asymptotic flatness

seem unable to allow stable stationary orbits. However, the black rings with a thickness less than a critical value admit stable stationary timelike geodesics even though the spacetimes have the five-dimensional asymptotic flatness [16, 17]. As for null geodesics around a black hole, it is well known that there exist unstable circular orbits of massless particles in four dimensions. The unstable circular orbits can be generalized in the higher-dimensional asymptotically flat spherical black hole cases. As far as we know, no stable bound null geodesic orbit around a gravitating body in an asymptotically flat spacetime was reported in any dimensions. The result in the present paper is the first example of the orbits of massless particles that are stably bound by the gravitational field outside a black object.

A fat black ring whose thickness is larger than the critical value  $\nu_c$  cannot bind any massless particles stably. Therefore, if the black ring that binds massless particles stably at an initial stage becomes fat with  $\nu > \nu_c$  by absorbing free-falling energy, then some part of the massless particles would be released toward infinity as radiation. This radiation would be a typical phenomenon for black rings, not for black holes. Furthermore, since the stationary points of the effective potential that allow stable bound orbits of massless particles are local minima, then massless particles trapped in a potential well outside the horizon can escape outward by quantum tunneling.

It is also an interesting question whether nonstationary bounded motion of massless particles in black ring spacetimes is chaotic or not. In the previous paper [17], we show an evidence of chaotic motion of massive particles by using Poincaré map. It suggests black rings allow no additional Killing tensor other than evidently known Killing vectors. Detailed investigations for null geodesics are important in relation to the conformal Killing tensor.

### Acknowledgements

This work is supported by Grant-in-Aid for JSPS No.J111000492 (T.I.) and Grant-in-Aid for Scientific Research No.19540305 (H.I.).

### Appendix A: Conditions of the critical value $\nu_c$

As discussed in Sec. III, there exist stable toroidal spiral orbits of massless particles, satisfying Eqs. (17), (18), and (20), if  $\nu$  is smaller than  $\nu_c$ . As marginally stable toroidal spiral orbits, there exist the innermost stable toroidal spiral orbit (ISTSO) and the outermost stable toroidal spiral

orbit (OSTSO), satisfying

$$\det \mathcal{H}(U)|_{\Sigma} = 0. \quad (\text{A1})$$

Hence, the Hessian matrix  $\mathcal{H}(U)|_{\Sigma}$  has a zero-eigenvalue, or equivalently, the effective potential has a flat direction, i.e.,

$$\partial_{\sigma}^2 U = 0 \quad (\text{A2})$$

at the ISTSO and the OSTSO, where  $\partial_{\sigma}$  is the eigenvector of  $\mathcal{H}(U)|_{\Sigma}$  associated with the zero-eigenvalue.

If  $\nu$  increases to  $\nu_c$ , the ISTSO and the OSTSO approach each other, and they degenerate in the limit  $\nu = \nu_c$ . At the degenerate stationary point, the condition

$$\partial_{\sigma}(\det \mathcal{H}) = 0, \quad (\text{A3})$$

or equivalently,

$$\partial_{\sigma}^3 U = 0 \quad (\text{A4})$$

holds. The five conditions (17), (18), (A1), and (A3) determine  $\nu_c$  and  $(\zeta, \rho, l_{\psi}, l_{\phi})$  for the degenerate point.

- 
- [1] R. Emparan and H. S. Reall, Living Rev. Relativity **11**, (2008).
  - [2] R. C. Myers and M. J. Perry, Annals Phys. **172**, 304 (1986).
  - [3] R. Emparan and H. S. Reall, Phys. Rev. Lett. **88**, 101101 (2002)
  - [4] A. A. Pomeransky and R. A. Sen'kov, hep-th/0612005.
  - [5] T. Mishima and H. Iguchi, Phys. Rev. D **73**, 044030 (2006).
  - [6] H. Elvang and P. Figueras, JHEP **0705**, 050 (2007).
  - [7] H. Iguchi and T. Mishima, Phys. Rev. D **75**, 064018 (2007) [Erratum-ibid. D **78**, 069903 (2008)].
  - [8] J. Evslin and C. Krishnan, Class. Quant. Grav. **26**, 125018 (2009).
  - [9] K. Izumi, Prog. Theor. Phys. **119**, 757 (2008).
  - [10] H. Elvang and M. J. Rodriguez, JHEP **0804**, 045 (2008).
  - [11] V. P. Frolov and D. Stojkovic, Phys. Rev. D **68**, 064011 (2003).
  - [12] J. Hoskisson, Phys. Rev. D **78**, 064039 (2008).
  - [13] M. Durkee, Class. Quant. Grav. **26**, 085016 (2009).
  - [14] S. Grunau, V. Kagramanova, J. Kunz and C. Lammerzahl, Phys. Rev. D **86**, 104002 (2012).

- [15] S. Grunau, V. Kagramanova and J. Kunz, arXiv:1212.0416 [gr-qc].
- [16] T. Igata, H. Ishihara and Y. Takamori, Phys. Rev. D **82**, 101501 (2010).
- [17] T. Igata, H. Ishihara and Y. Takamori, Phys. Rev. D **83**, 047501 (2011).
- [18] P. Dobiasch and D. Maison, Gen. Rel. Grav. **14**, 231 (1982).
- [19] G. W. Gibbons and D. L. Wiltshire, Annals Phys. **167**, 201 (1986) [Erratum-ibid. **176**, 393 (1987)].
- [20] H. Ishihara and K. Matsuno, Prog. Theor. Phys. **116**, 417 (2006).
- [21] K. Matsuno and H. Ishihara, Phys. Rev. D **80**, 104037 (2009).